

DD-MIC(0) preconditioning of rotated trilinear FEM elasticity systems

I. Georgiev, S. Margenov

Central Laboratory of Parallel Processing,
Bulgarian Academy of Sciences,
Acad. G. Bontchev str., B1.25/7, 1113 Sofia, Bulgaria

(Received December 13, 2002)

New results about preconditioning of rotated trilinear nonconforming FEM elasticity systems in the case of mesh anisotropy are presented. The solver of the arising linear system is based on the constructed efficient preconditioner of the coupled stiffness matrix. Displacement decomposition of the stiffness matrix is used as a first step of the algorithm. At the second step, modified incomplete factorization MIC(0) with perturbation is applied to a proper auxiliary M-matrix to get an approximate factorization of the obtained block-diagonal matrix. The derived condition number estimates and the presented numerical tests well illustrate the behaviour of the theoretically studied algorithms as well as their robustness for some more realistic benchmark problems.

1. INTRODUCTION

Nonconforming finite elements based on *rotated* multilinear shape functions were introduced by Rannacher and Turek [11] as a class of simple elements for the Stokes problem. More generally, the recent activities in the development of efficient solution methods for nonconforming finite element systems are inspired by their attractive properties as a stable discretization tools for ill-conditioned problems including the case of strong coefficient jumps. Such a situation is typical for problems related to computer simulation of foundation systems in weak soil layers. This paper is focused on the numerical solution of the Lamé equations of elasticity strongly motivated by the attractive sparsity of the corresponding stiffness matrices which regular structure holds even in the case of non-regular meshes. Two algorithms are presented, where *MP* and *MV* stand for the variants of the nodal basis functions corresponding to midpoint and integral midvalue interpolation operators.

Let us consider the weak formulation of the linear elasticity problem in the form: find $\underline{u} \in [H_E^1(\Omega)]^3 = \{v \in [H^1(\Omega)]^3 : \underline{v}|_{\Gamma_D} = \underline{u}_S\}$ such that

$$\int_{\Omega} [2\mu \varepsilon(\underline{u}) : \varepsilon(\underline{v}) + \lambda \operatorname{div} \underline{u} \operatorname{div} \underline{v}] \, d\Omega = \int_{\Omega} \underline{f}^t \underline{v} \, d\Omega + \int_{\Gamma_N} \underline{g}_S^t \underline{v} \, d\Gamma, \quad (1)$$

$\forall \underline{v} \in [H_0^1(\Omega)]^3 = \{v \in [H^1(\Omega)]^3 : \underline{v}|_{\Gamma_D} = 0\}$, with the positive constants λ and μ of Lamé, the symmetric strains

$$\varepsilon(\underline{u}) := 0.5(\nabla \underline{u} + (\nabla \underline{u})^t),$$

the volume forces \underline{f} , and the boundary tractions \underline{g} .

The construction of robust nonconforming FEM methods are generally based on application of mixed formulation for \underline{u} and $\operatorname{div} \underline{u}$ to obtain a stable saddle-point system. By the choice of non continuous finite elements for the dual variable, it can be eliminated at the (macro)element level, and we get a symmetric positive definite FEM system in primal (displacements) variables. This approach is known as *reduced and selective integration*(RSI) technique, see [8].

Let $\Omega^H = \omega_1^H \times \omega_2^H \times \omega_3^H$ be a regular coarser decomposition of the domain $\Omega \subset \mathbf{R}^3$ into (convex) hexahedrons denoted by \mathcal{E} , and let the finer decomposition $\Omega^h = \omega_1^h \times \omega_2^h \times \omega_3^h$ be obtained by a regular refinement of the macroelements $\mathcal{E} \in \Omega^H$ into eight similar hexahedrons denoted by e . In defining the isoparametric rotated trilinear element, one uses the unit cube (with edges parallel to the coordinate axes) as a reference element \hat{e} . For each $e \in \Omega^h$, let $\psi_e : \hat{e} \rightarrow e$ be the corresponding trilinear transformation. The element nodal basis functions are determined by the relations

$$\{\phi_i\}_{i=1}^6 = \{\hat{\phi}_i \circ \psi_e^{-1}\}_{i=1}^6,$$

where $\hat{\phi}_i \in \text{span}\{1, \xi_j, \xi_j^2 - \xi_{j+1}^2, j = 1, 2, 3\}$, and ‘o’ denote the composition of functions $\hat{\phi}_i$ and ψ_e^{-1} . For the algorithm *MP*, the reference element basis functions $\{\hat{\phi}_i\}_{i=1}^6$ are determined by the standard interpolation conditions

$$\hat{\phi}_i(b_\Gamma^j) = \delta_{ij},$$

where $\{b_\Gamma^j\}_{j=1}^6$ are the midpoints of the walls $\{\Gamma_\hat{e}^j\}_{j=1}^6$ of \hat{e} , and then

$$\{\hat{\phi}_i\}_{i=1}^6 = \{(1 \pm 3\xi_j + 2\xi_j^2 - \xi_{j+1}^2 - \xi_{j+2}^2) / 6, j = 1, 2, 3\}.$$

Alternatively, for the algorithm *MV*, integral midvalue interpolation operator is applied in the form

$$|\Gamma_\hat{e}^j|^{-1} \int_{\Gamma_\hat{e}^j} \hat{\phi}_i = \delta_{ij},$$

and then

$$\{\hat{\phi}_i\}_{i=1}^6 = \{(2 \pm 6\xi_j + 6\xi_j^2 - 3\xi_{j+1}^2 - 3\xi_{j+2}^2) / 12, j = 1, 2, 3\}.$$

Now, the non-conforming FEM space V_E^h is defined as follows

$$V_E^h = \left\{ \underline{v}^h \in [L^2(\Omega)]^3 : \underline{v}^h|_e = \sum_{i=1}^6 \underline{v}^h(x_{e,i}) \phi_i, \forall e \in \Omega^h, \underline{v}_h(b_e, \Gamma_D) = \underline{u}_S(b_e, \Gamma_D) \right\}.$$

Here $x_{e,i}$ is the current midpoint/node of the hexahedron faces, and b_{e,Γ_D} stands for the midpoint of the related element face Γ if $\Gamma \subset \Gamma_D$. Let us denote also by V_0^h the FEM space, satisfying (in a nodalwise sense) homogeneous boundary conditions on Γ_D .

We consider a RSI FEM discretization of the problem written in the form: find $\underline{u}^h \in V_E^h$ such that

$$\sum_{e \in \Omega^h} \int_e \left[2\mu \varepsilon^*(\underline{u}^h) : \varepsilon^*(\underline{v}^h) + \lambda \text{div } \underline{u}^h \text{ div } \underline{v}^h \right] de = \int_\Omega \underline{f}^t \underline{v}^h \Omega + \int_{\Gamma_N} \underline{g}_S^t \underline{v}^h d\Gamma, \tag{2}$$

$\forall \underline{v}^h \in V_0^h$, where

$$\varepsilon^*(\underline{u}) := \nabla \underline{u} - 0.5 I_L^{QH} [\nabla \underline{u} - (\nabla \underline{u})^t].$$

The operator I_L^{QH} denotes the L_2 -orthogonal projection onto Q^H , the space of piecewise constant functions on the coarser decomposition Ω^H of Ω . The introduced variational problem (2) can be considered as a generalization of the related 2D formulation studied, e.g., in [5]. It was first introduced in [9] (see also [10]).

It is important to note that the straightforward low order, nonconforming FEM discretization of the elasticity problem (1) is ill posed since the obtained discrete problem does not satisfy the Korn’s

second inequality. This disadvantage is overcome in (2) by the I_L^{QH} projection which is equivalent to a mixed formulation with respect to the space pair $(V_E^h \times Q^H)$.

Applying the RSI FEM discretization (2) we get the linear algebraic system

$$Ku = f \quad (3)$$

where K is the related symmetric and positive definite stiffness matrix. Let us assume that K is written in a 3×3 block form

$$K = \begin{bmatrix} K_{11} & K_{12} & K_{13} \\ K_{21} & K_{22} & K_{23} \\ K_{31} & K_{32} & K_{33} \end{bmatrix},$$

where the block structure corresponds to a separate displacement component ordering of the vector of nodal unknowns. Our aim is to develop an efficient solution method for the system (3) suitable for large-scale and very large-scale problems.

For preconditioning of K we use the isotropic variant of the displacement decomposition (DD) approach, see e.g. [2, 4], where the preconditioner C_{DD} is written as follows

$$C_{DD} = \begin{bmatrix} \tilde{A} & & \\ & \tilde{A} & \\ & & \tilde{A} \end{bmatrix}, \quad (4)$$

with a proper approximation (preconditioner) \tilde{A} of the stiffness matrix A corresponding to the bilinear form

$$a(u^h, v^h) = \sum_{e \in \Omega^h} \int_e E \left(\sum_{i=1}^3 \frac{\partial u^h}{\partial x_i} \frac{\partial v^h}{\partial x_i} \right) de. \quad (5)$$

Such preconditioning of the coupled matrix K is theoretically motivated by the Korn's inequality which holds for the RSI FEM discretization (2) under consideration.

2. DD MIC(0) PRECONDITIONING

In this section we recall some known facts about the modified incomplete factorization MIC(0) preconditioner applied to the matrix A (see (4)). Our presentation at this point follows those from [4]; see [12] for an alternative approach. Let us rewrite the real $N \times N$ matrix $A = (a_{ij})$ in the form

$$A = D - L - L^t, \quad (6)$$

where D is the diagonal and $(-L)$ is the strictly lower triangular part of A . Then we consider the approximate factorization of A which has the following form

$$C_{MIC(0)} = (X - L)X^{-1}(X - L)^t,$$

where $X = \text{diag}(x_1, \dots, x_N)$ is a diagonal matrix determined by the condition of equal rowsums

$$C_{MIC(0)}\underline{e} = A\underline{e}, \quad \underline{e} = (1, \dots, 1)^t \in \mathcal{R}^N.$$

For the purpose of preconditioning, we are interested in the case when $X > 0$ and thus $C_{MIC(0)}$ is positive definite. If this holds, we speak about *stable* MIC(0) factorization. Concerning stability of MIC(0) factorization, we have the following theorem.

Theorem 1. Let $A = (a_{ij})$ be a symmetric real $N \times N$ matrix and let $A = D - L - L^t$ be the splitting (6) of A . Let us assume that

$$\begin{aligned} L &\geq 0, \\ A\mathbf{e} &\geq 0, \\ A\mathbf{e} + L^t\mathbf{e} &> 0, \quad \mathbf{e} = (1, \dots, 1)^t \in \mathcal{R}^N, \end{aligned}$$

i.e. that A is a weakly diagonally dominant matrix with nonpositive offdiagonal entries and that $A + L^t = D - L$ is strictly diagonally dominant.

Then the relation

$$x_i = a_{ii} - \sum_{k=1}^{i-1} \frac{a_{ik}}{x_k} \sum_{j=k+1}^N a_{kj}$$

gives the positive values x_i and the diagonal matrix $X = \text{diag}(x_1, \dots, x_N)$ defines stable $MIC(0)$ factorization of A .

Now we introduce the displacement decomposition incomplete factorization preconditioner $C_{DD \text{ MIC}(0)}$ in the form

$$C_{DD \text{ MIC}(0)}(K) = \begin{bmatrix} \mathcal{C}_{MIC(0)}(A) & & \\ & \mathcal{C}_{MIC(0)}(A) & \\ & & \mathcal{C}_{MIC(0)}(A) \end{bmatrix}. \tag{7}$$

Here $\mathcal{C}_{MIC(0)}(A)$ stands for the $MIC(0)$ preconditioner of A . It is assumed that if (in the general case) the matrix A does not satisfy the stability conditions of the Theorem 1 it should be first modified in a proper way to a matrix allowing stable $MIC(0)$ factorization [12].

Remark 1. The numerical tests presented in the last section are performed using the perturbed version of $MIC(0)$ algorithm, where the incomplete factorization is applied to the matrix $\tilde{A} = A + \tilde{D}$. The diagonal perturbation $\tilde{D} = \tilde{D}(\xi) = \text{diag}(\tilde{d}_1, \dots, \tilde{d}_N)$ is defined as follows:

$$\tilde{d}_i = \begin{cases} \xi a_{ii} & \text{if } a_{ii} \geq 2w_i \\ \xi^{1/2} a_{ii} & \text{if } a_{ii} < 2w_i \end{cases}$$

where $0 < \xi < 1$ is a constant and $w_i = \sum_{j>i} -a_{ij}$.

3. LOCAL ANALYSIS

For the chosen (brick) finite element $e \in \Omega^h$, we introduce the local squares of ratios of mesh anisotropy $p = \min_{i,j} (h_i/h_j)^2$, $q = \max_{i,j} (h_i/h_j)^2$, $i, j \in \{1, 2, 3\}$, where h_i are the local mesh parameters, and let $r = \min_i h_i$. Then the element stiffness matrices corresponding to MP and MV variants of the rotated trilinear FEM read as follows:

$$A_{MP}^{(e)} = \frac{2a(e)r}{27\sqrt{pq}} \begin{pmatrix} a_{MP}^{11} & a_{MP}^{12} & a_{MP}^{13} \\ a_{MP}^{21} & a_{MP}^{22} & a_{MP}^{23} \\ a_{MP}^{31} & a_{MP}^{32} & a_{MP}^{33} \end{pmatrix},$$

$$a_{MP}^{11} = \begin{pmatrix} 43pq + 4q + 4p & -11pq + 4q + 4p \\ -11pq + 4q + 4p & 43pq + 4q + 4p \end{pmatrix},$$

$$a_{MP}^{22} = \begin{pmatrix} 4pq + 43q + 4p & -4pq - 11q + 4p \\ -4pq - 11q + 4p & 4pq + 43q + 4p \end{pmatrix},$$

$$a_{MP}^{33} = \begin{pmatrix} 4pq + 4q + 43p & 4pq - 4q - 11p \\ 4pq - 4q - 43p & 4pq + 4q + 43p \end{pmatrix},$$

$$a_{MP}^{12} = \begin{pmatrix} -8pq - 8q + 4p & -8pq - 8q + 4p \\ -8pq - 8q + 4p & -8pq - 8q + 4p \end{pmatrix},$$

$$a_{MP}^{13} = \begin{pmatrix} -8pq + 4q - 8p & -8pq + 4q - 8p \\ -8pq + 4q - 8p & -8pq + 4q - 8p \end{pmatrix},$$

$$a_{MP}^{23} = \begin{pmatrix} 4pq - 8q - 8p & 4pq - 8q - 8p \\ 4pq - 8q - 8p & 4pq - 8q - 8p \end{pmatrix},$$

$$A_{MV}^{(e)} = \frac{2a(e)r}{3\sqrt{pq}} \begin{pmatrix} a_{MV}^{11} & a_{MV}^{12} & a_{MV}^{13} \\ a_{MV}^{21} & a_{MV}^{22} & a_{MV}^{23} \\ a_{MV}^{31} & a_{MV}^{32} & a_{MV}^{33} \end{pmatrix},$$

$$a_{MV}^{11} = \begin{pmatrix} 7pq + q + p & pq + q + p \\ pq + q + p & 7pq + q + p \end{pmatrix},$$

$$a_{MV}^{22} = \begin{pmatrix} pq + 7q + p & pq + q + p \\ pq + q + p & pq + 7q + p \end{pmatrix},$$

$$a_{MV}^{33} = \begin{pmatrix} pq + q + 7p & pq + q + p \\ pq + q + p & pq + q + 7p \end{pmatrix},$$

$$a_{MV}^{12} = \begin{pmatrix} -2pq - 2q + p & -2pq - 2q + p \\ -2pq - 2q + p & -2pq - 2q + p \end{pmatrix},$$

$$a_{MV}^{13} = \begin{pmatrix} -2pq + q - 2p & -2pq + q - 2p \\ -2pq + q - 2p & -2pq + q - 2p \end{pmatrix},$$

$$a_{MV}^{23} = \begin{pmatrix} pq - 2q - 2p & pq - 2q - 2p \\ pq - 2q - 2p & pq - 2q - 2p \end{pmatrix}.$$

Lemma 1. The element stiffness matrix for algorithm MP is M-matrix if and only if $(p, q) \in T$, where the curvilinear triangle T is given by

$$T = \left\{ \begin{array}{l} p \in (4/7, 1) : \frac{4p}{11p-4} \leq q \leq \frac{11p}{4(p+1)} \\ p \in (1, 7/4) : \frac{4p}{11-4p} \leq q \leq \frac{11p}{4(p+1)} \end{array} \right\}.$$

The element stiffness matrix for algorithm MV is never M-matrix.

The global stiffness matrix can be written in the form $A = \sum_e A^{(e)}$ where the sum stands for the standard FEM assembling procedure. We will analyze here two constructions of auxiliary M-matrices to be used as a preliminary preconditioning step of A . We will first introduce $\bar{B}_1 = \sum_e \bar{B}_1^{(e)}$

where the element stiffness matrix $\bar{B}_1^{(e)}$ corresponds to MP algorithm in $[-h, h]^3$, namely

$$\bar{B}_1^{(e)} = \frac{2a(e)h}{9} \begin{bmatrix} 17 & -1 & -4 & -4 & -4 & -4 \\ -1 & 17 & -4 & -4 & -4 & -4 \\ -4 & -4 & 17 & -1 & -4 & -4 \\ -4 & -4 & -1 & 17 & -4 & -4 \\ -4 & -4 & -4 & -4 & 17 & -1 \\ -4 & -4 & -4 & -4 & -1 & 17 \end{bmatrix}.$$

In the second option, we use $\bar{B}_2 = \sum_e \bar{B}_2^{(e)}$, where the element matrix $\bar{B}_2^{(e)}$ is obtained from the original matrix $A^{(e)}$ by simply zeroing the positive offdiagonal entries, and then modifying the diagonal to fulfill the rowsum criteria, see [7]. Here a detailed local spectral analysis for the first variant is presented. The eigenvalues of the generalized eigenvalue problem

$$A_{MP}^{(e)} u = \lambda \bar{B}_1^{(e)} u$$

are as follows

$$\lambda_1 = \frac{p}{\sqrt{pq}}, \quad \lambda_2 = \frac{q}{\sqrt{pq}}, \quad \lambda_3 = \frac{pq}{\sqrt{pq}},$$

$$\lambda_{4,5} = \frac{1}{3} \frac{(pq + p + q) \pm \sqrt{(pq + p + q)^2 - 3pq(p + q + 1)}}{\sqrt{pq}},$$

and respectively for the algorithm MV

$$A_{MV}^{(e)} u = \lambda \bar{B}_1^{(e)} u,$$

$$\lambda_1 = \frac{p}{\sqrt{pq}}, \quad \lambda_2 = \frac{q}{\sqrt{pq}}, \quad \lambda_3 = \frac{pq}{\sqrt{pq}},$$

$$\lambda_{4,5} = \frac{3}{4} \frac{(pq + p + q) \pm \sqrt{(pq + p + q)^2 - 3pq(p + q + 1)}}{\sqrt{pq}}.$$

Similar results are obtained for second variant where the same eigenproblems with $\bar{B}_2^{(e)}$ in the right hand side are solved.

Now, let us locally modify the introduced matrices $\bar{B}_k^{(e)}$. The following readily seen lemma will be used to get the final results of this section.

Lemma 2. Let us define B_k , $k = 1, 2$ in the form

$$B_k = \sum_e \frac{1}{\lambda_{\min}^{(e)}} \bar{B}_k^{(e)}, \quad k = 1, 2.$$

Then the relative condition number of this locally scaled preconditioning matrix satisfy the estimate

$$\kappa \left((B_k)^{-1} A \right) \leq \max_e \kappa \left(\left(B_k^{(e)} \right)^{-1} A^{(e)} \right) = \max_e \frac{\lambda_{\max}^{(e)}}{\lambda_{\min}^{(e)}}.$$

Theorem 2. Let us denote by Q the maximal of the locally introduced parameters of mesh anisotropy q , that is

$$Q = \max_e q.$$

Then the following estimates for the relative condition numbers hold (see [6]):

$$\kappa \left((B_1^{MP})^{-1} A_1^{MP} \right) \leq Q, \quad \kappa \left((B_2^{MP})^{-1} A_2^{MP} \right) \leq \frac{9}{4} Q,$$

$$\kappa \left((B_1^{MV})^{-1} A_1^{MV} \right) \leq \frac{1}{2} (Q + 1), \quad \kappa \left((B_2^{MV})^{-1} A_2^{MV} \right) \leq \frac{4}{3} (Q + 1).$$

In the end, we obtain our preconditioners by $MIC(0)$ factorization of the introduced auxiliary matrices B_k^{MP} and B_k^{MV} , $k = 1, 2$.

Remark 2. The local scaling procedure is simple but very important, especially in the case of varying directions of dominating mesh anisotropy.

Remark 3. The general conclusion is that the proposed algorithms are suitable for problems with moderate mesh anisotropy. Advantages of the first variant could be considered, because the estimates for the condition number are better.

4. COMPUTATIONAL COMPLEXITY

The Preconditioned Conjugate Gradient (PCG) algorithm for solution of the linear system

$$K\mathbf{u} = \mathbf{b}$$

can be written as follows (see [1]):

given \mathbf{u}^0

compute $\mathbf{g}^0 = \mathbf{b} - K\mathbf{u}^0$, $\mathbf{h}^0 = C^{-1}\mathbf{g}^0$, $\mathbf{d}^0 = \mathbf{h}^0$

for $i = 0, 1, 2, \dots$ until $\|\mathbf{g}^i\| \leq \epsilon\|\mathbf{g}^0\|$ do

$$\tau_i = \langle \mathbf{g}^i, \mathbf{h}^i \rangle / \langle K\mathbf{d}^i, \mathbf{d}^i \rangle,$$

$$\mathbf{u}^{i+1} = \mathbf{u}^i + \tau_i \mathbf{d}^i,$$

$$\mathbf{g}^{i+1} = \mathbf{g}^i - \tau_i K\mathbf{d}^i,$$

$$\mathbf{h}^{i+1} = C^{-1}\mathbf{g}^{i+1},$$

$$\beta_i = \langle \mathbf{g}^{i+1}, \mathbf{h}^{i+1} \rangle / \langle \mathbf{g}^i, \mathbf{h}^i \rangle,$$

$$\mathbf{d}^{i+1} = \mathbf{h}^{i+1} + \beta_i \mathbf{d}^i$$

enddo

We analyze here the computational complexity \mathcal{N}^{it} of one PCG iteration. It is easy to see that

$$\mathcal{N}^{it} = 2\mathcal{N}(\langle \cdot, \cdot \rangle) + 3\mathcal{N}_{LT} + \mathcal{N}(K\mathbf{x}) + \mathcal{N}(C^{-1}\mathbf{x}), \quad (8)$$

where $\mathcal{N}(\langle \cdot, \cdot \rangle)$, \mathcal{N}_{LT} , $\mathcal{N}(K\mathbf{x})$, and $\mathcal{N}(C^{-1}\mathbf{x})$ stand respectively for the computational complexity of the inner product, one linked triad of the form $\mathbf{x} = \mathbf{y} + \alpha\mathbf{z}$, the stiffness matrix vector multiplication, and the solution of a linear system with the preconditioning matrix C .

Next we will assume that the mesh is (topo)logically equivalent to the uniform mesh in the unit cube with mesh size $h = h_i$, $i = 1, 2, 3$ and the number of intervals in each coordinate direction is equal to n . This means that the size of the stiffness matrix K is $N = 9(n+1)n^2$.

The contribution of the first three terms of \mathcal{N}_{it} does not depend of the preconditioner, and can be written in the form

$$\begin{aligned} 2\mathcal{N}(\langle \cdot, \cdot \rangle) + 3\mathcal{N}_{LT} &= 10N + \dots \\ \mathcal{N}(K\mathbf{x}) &= 407N + \dots \end{aligned} \quad (9)$$

where only the leading term with respect to N is explicitly given. We would now turn the attention of the reader towards the relatively large number ($3 \times 68 = 204$) of the non-zero entries per row of the stiffness matrix K which is due to the I_L^{QH} projection term of the stabilized RSI FEM formulation (2) of the problem.

To complete this analysis we derive estimates of the computational complexity of the solution of a linear system with the introduced displacement decomposition preconditioner:

$$\mathcal{N}(C_{DD\text{ MIC}(0)}^{-1}\mathbf{x}) = 21N + \dots \quad (10)$$

Combining (8), (9) and (10) we get the final computational complexity estimates per iteration in the form:

$$\mathcal{N}_{DD\text{ MIC}(0)}^{it} = 438N + \dots \quad (11)$$

At the end of this section we consider the important particular case of a rectangular brick mesh where the number of intervals equal to n in each coordinate direction. This means that the macroelements are parallelepipeds divided into eight subparallelepipeds. We can separate the nodes of the

macroelement in two groups: interior nodes and nodes belonging to the macroelement walls. Taking into account that different nodes have different contribution in the macroelement matrix we can calculate that the average number of the non-zero entries per row is equal to 27 and hence

$$\begin{aligned} \mathcal{N}(K^{(um)} \underline{x}) &= 53N + \dots \\ \mathcal{N}_{DD \text{ MIC}(0)}^{(um)} &= 84N + \dots \end{aligned} \quad (12)$$

The superscript um in (12) stands for the case of $(u)ni$ form $(m)esh$.

5. BENCHMARKING

The presented numerical tests illustrate the PCG convergence rate of the studied displacement decomposition algorithms when the size of the discrete problem, the coefficient jumps and the mesh anisotropy are varied. A special attention is given to the simulation of the stressed-strained state of a pile in a weak soil layer where also a locally refined mesh is considered.

The computational domain is the parallelepiped $\Omega = \Delta_x \times \Delta_y \times \Delta_z$ where homogeneous Dirichlet boundary conditions are assumed at the bottom face. A uniform mesh is used, where accordingly to the RSI FEM discretization (2) of the elasticity problem, the coarser grid and the finer grid parameters are respectively $H_i, h_i, i = 1, 2, 3$. The number of intervals in each of the coordinate directions for the coarse grid is equal to m and respectively for the finer grid $n = 2m$. The size of the resulting non-conforming FEM system is $N = 9n^2(n + 1)$.

A relative stopping criterion $(C^{-1} r^{N_{it}}, r^{N_{it}})/(C^{-1} r^0, r^0) < \varepsilon^2$ is used in the PCG algorithm, where r^i stands for the residual at the i -th iteration step, and $\varepsilon = 10^{-3}$.

Benchmark 1. Computer simulation of the stressed-strained state of a soil body under a *square footing* is considered. The volume forces are assumed equal to zero with a vertical external load which is uniformly distributed across the square seal $|S| = H_x \times H_y$, (see Fig. 1(a)).

The mechanical characteristics $E_s = 10$ MPa and $\nu_s = 0.35$ correspond to a *softly plastic clay* layer. The related numerical results are given in Tables 1 and 2. What we clearly observe is the stable behavior of the PCG algorithm. The obtained test data fully confirm the expected asymptotic of iterations $N_{it} = O(Q^{1/2})$.

Table 1. Benchmark 1. PCG iterations: algorithm MP

$m = n/2$	N	variant 1				variant 2			
		(p, q)				(p, q)			
		(1,1)	(1,4)	(1,16)	(1,64)	(1,1)	(1,4)	(1,16)	(1,64)
3	2 268	37	62	79	160	37	58	58	119
7	26 460	54	96	131	291	54	65	105	145
15	251 100	77	137	188	438	77	79	155	192
31	2 179 548	106	190	262	626	106	125	216	309

Table 2. Benchmark 1. PCG iterations: algorithm MV

$m = n/2$	N	variant 1				variant 2			
		(p, q)				(p, q)			
		(1,1)	(1,4)	(1,16)	(1,64)	(1,1)	(1,4)	(1,16)	(1,64)
3	2 268	42	72	129	191	42	69	120	137
7	26 460	66	119	165	361	65	117	130	274
15	251 100	95	171	235	546	94	171	194	442
31	2 179 548	134	240	328	784	132	242	271	637

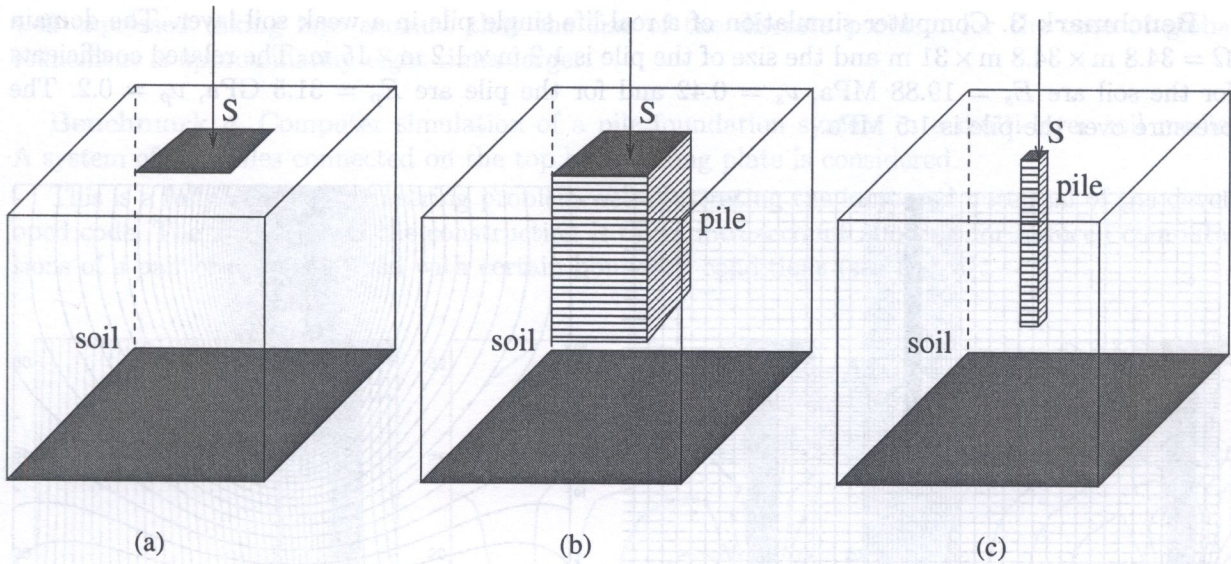


Fig. 1. (a) Squire footing: BM1; (b) Foundation element: BM2($m = 3$); (c) Foundation element: BM2($m = 15$)

Benchmark 2. The interaction between a soil media and a given model of foundation element with varying elasticity modulus is considered.

The geometry is similar to this in Benchmark 1 (see Fig. 1(b)-(c)). The characteristics of the foundation are $E_p \in \{10 \text{ MPa}, 100 \text{ MPa}, 1000 \text{ MPa}, 10\,000 \text{ MPa}\}$ and $\nu_p = 0.2$ while these of the soil are as in Benchmark 1. A vertical external load is applied uniformly distributed across the top side of the foundation. In the finest grid case, i.e. when $m=31$, and when $E_p = 10\,000 \text{ MPa}$, this benchmark could be associated with computer simulation of a single pile in a weak soil layer. The results for Benchmark 2 are presented in Tables 3 and 4. Here, one can observe how the preconditioning algorithm behaves when the coefficient jump varies, and when in addition, the size of the included foundation element decreases with the mesh parameters H_x and H_y . This benchmark well illustrates the features of the method and the related algorithms when the coefficient jumps are extremely (based on the mesh size) local.

Table 3. Benchmark 2. PCG iterations: algorithm MP, variant 2

$m = n/2$	N	$(p, q) = (1, 1)$			$(p, q) = (2, 1)$			$(p, q) = (4, 1)$		
		$E_p = 100$	$E_p = 1000$	$E_p = 10000$	$E_p = 100$	$E_p = 1000$	$E_p = 10000$	$E_p = 100$	$E_p = 1000$	$E_p = 10000$
3	2 268	51	88	111	49	112	144	55	97	124
7	26 460	65	143	186	53	115	268	69	146	252
15	251 100	86	193	289	90	123	319	88	172	378
31	2 179 548	116	229	393	156	195	344	119	194	477

Table 4. Benchmark 2. PCG iterations: algorithm MV, variant 2

$m = n/2$	N	$(p, q) = (1, 1)$			$(p, q) = (2, 1)$			$(p, q) = (4, 1)$		
		$E_p = 100$	$E_p = 1000$	$E_p = 10000$	$E_p = 100$	$E_p = 1000$	$E_p = 10000$	$E_p = 100$	$E_p = 1000$	$E_p = 10000$
3	2 268	56	91	124	59	115	149	62	133	172
7	26 460	76	132	210	75	167	255	89	204	324
15	251 100	106	173	355	101	180	413	115	217	478
31	2 179 548	145	210	490	136	207	509	150	241	615

Benchmark 3. Computer simulation of a real-life single pile in a weak soil layer. The domain $\Omega = 34.8 \text{ m} \times 34.8 \text{ m} \times 31 \text{ m}$ and the size of the pile is $1.2 \text{ m} \times 1.2 \text{ m} \times 15 \text{ m}$. The related coefficients for the soil are $E_s = 19.88 \text{ MPa}$, $\nu_s = 0.42$ and for the pile are $E_p = 31.5 \text{ GPa}$, $\nu_p = 0.2$. The pressure over the pile is 1.5 MPa .

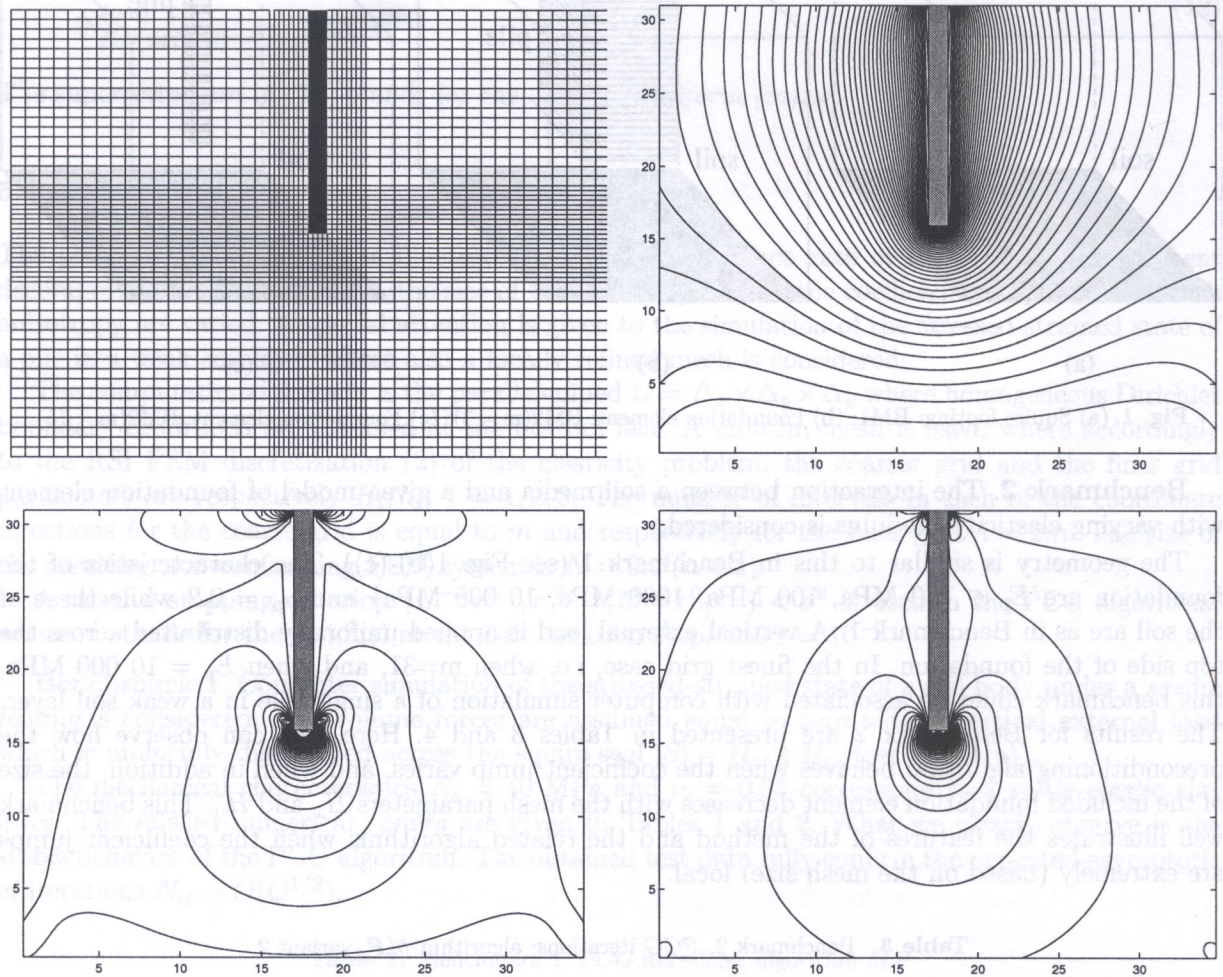


Fig. 2. Benchmark 3: Local refinement around the pile, vertical displacements, vertical stresses, vertical strains; cross section $y = 17.9 \text{ m}$

The locally refined mesh (see Fig. 2) is constructed so that the size of the discrete problem is the same as for so called coarse grid ($m_x = m_y = m_z = 29$). The locally refined subdomain corresponds to the *a priori* known zone of biggest gradients of the solution due to the strong coefficient jump which corresponds to the zone of strongest interactions between the concrete pile body and the surrounding soil layer.

We also consider a global regiment with factor two ($m_x = m_y = m_z = 58$). The numerical results for this benchmark are presented in Table 5. The computational efficiency of the local regiment is

Table 5. Benchmark 3. PCG iterations

algorithm	variant	coarse grid	local refinement	global refinement
AMP	1	455	913	845
	2	537	619	658
AMV	1	538	1085	990
	2	652	948	918

well expressed taking into account that the size of the discrete problem for the case of global refinement is approximately eight times larger.

Benchmark 4. Computer simulation of a pile foundation system in a multi-layer soil media. A system of four piles connected on the top by a linking plate is considered.

This is a fully real-life engineering problem well illustrating the increased potential of the developed code. The symmetry of the construction is taken into account allowing for reduced computations of a pair of piles equipped with certain boundary conditions (see Fig. 4).

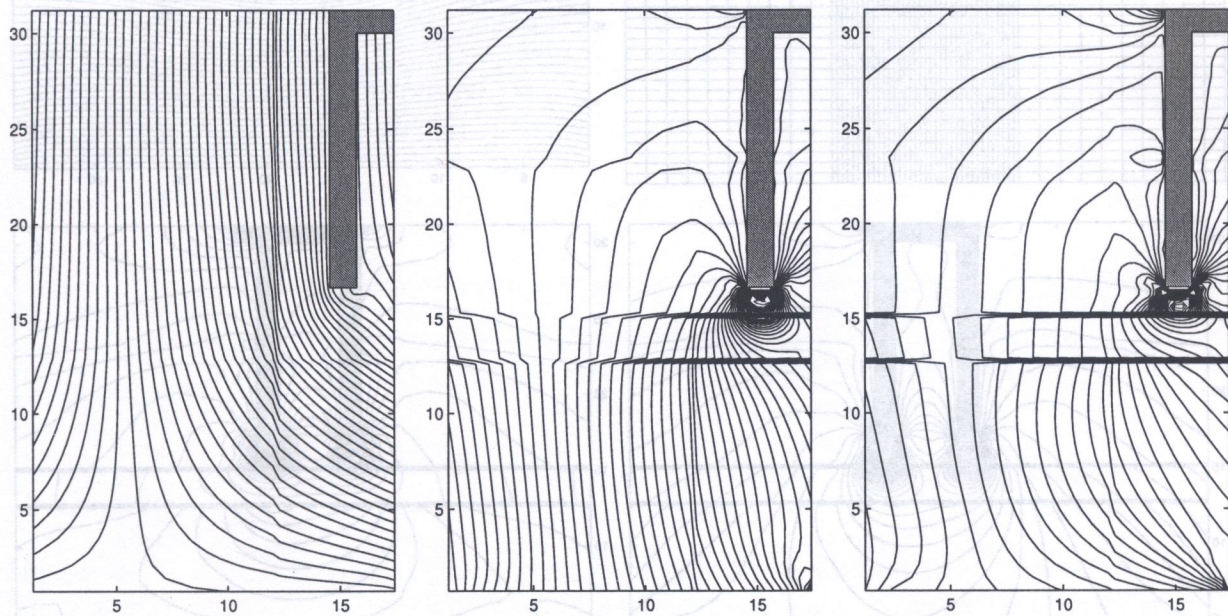


Fig. 3. Benchmark 4: first pile; vertical displacements, strains and stresses; cross section $x = 15.00$ m.

The computational domain is the parallelogram $\Omega = 34.8 \text{ m} \times 17.4 \text{ m} \times 31 \text{ m}$. The boundary conditions are as follows: homogeneous Dirichlet boundary conditions on the bottom side; homogeneous Neumann boundary conditions on the vertical sides; and nonhomogeneous Neumann boundary conditions on the top cross sections of the piles represent the loads of $V_1 = 2000 \text{ kN}$, $V_2 = 4000 \text{ kN}$ and $H_1 = H_2 = 150 \text{ kN}$, coming from the upper bridge construction. The subscript here indicate the number of piles where first is the left one. The soil media consists of four layers numbered towards up-to down and determined by the following mechanical characteristics: $E_{s1} = 20 \text{ MPa}$, $\nu_{s1} = 0.4$; $E_{s2} = 11 \text{ MPa}$, $\nu_{s2} = 0.35$; $E_{s3} = 7 \text{ MPa}$, $\nu_{s3} = 0.25$; $E_{s4} = 4.6 \text{ MPa}$, $\nu_{s4} = 0.2$. The mesh is properly refined around the piles. The presented selected set of plots well represent the complex spatial behaviour of the computed stressed-strained state of the interaction between the pile system and the surrounding multi-layer soil media, see Figs. 3 and 4.

Concluding Remarks: The analysis of the numerical tests confirms the robustness of the developed new algorithms and codes. The research team considers the obtained results as very prospective. One of the important steps in this field is to implement the accumulated *know how* to the numerical solution of coupled thermo-hydro-mechanical problems. Such a proposition is strongly motivated by the stable approximation properties of the nonconforming FEM with respect to all of the included phenomena. Such a complex treatment could be of a serious importance for various large scale engineering problems including such related to the foundation systems under complicated geological conditions. Another practical problem of great importance, described by the same mathematical model, is related to the long-term perspective study of the behaviour of nuclear waste repositories.

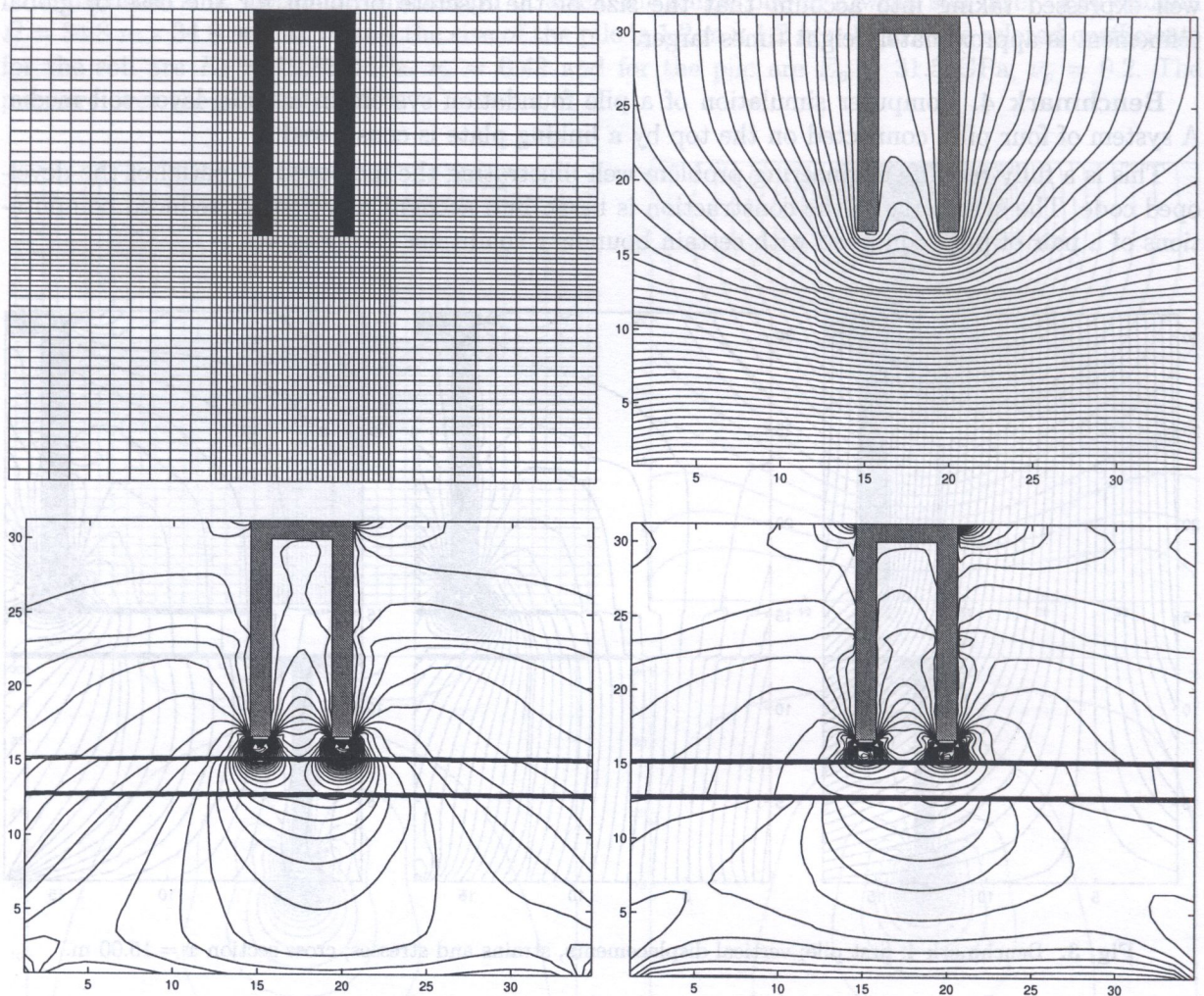


Fig. 4. Benchmark 4: Local refinement around the piles, vertical displacements, vertical stresses, vertical strains; cross section $y = 15.40$ m

ACKNOWLEDGMENT

Supported by Ministry of Education and Science of Bulgaria under Grant # MM 801/98 and Center of Excellence BIS-21 grant ICA1-2000-70016

REFERENCES

- [1] O. Axelsson. *Iterative Solution Methods*. University Press, Cambridge 1996.
- [2] O. Axelsson, I. Gustafsson. Iterative methods for the Navier equations of elasticity. *Comp. Meth. Appl. Mech. Engin.*, **15**: 241–258, 1978.
- [3] R. Beauwens, Y. Notay. *Efficient block preconditioning of elasticity problems*. Technical Report GANMN 98-01, Université Libre de Bruxelles, Brussels, Belgium 1998.
- [4] R. Blaheta. Displacement decomposition – incomplete factorization preconditioning techniques for linear elasticity problems. *Numer. Lin. Alg. Appl.*, **1**: 107–126, 1994.
- [5] R.S. Falk. Nonconforming finite element methods for the equations of linear elasticity. *Math. Comp.*, **57**: 529–550, 1991.
- [6] I. Georgiev, S. Margenov. MIC(0) preconditioning of rotated trilinear FEM elliptic systems. In: *Large-Scale Scientific Computing*, Lecture Notes in Computer Sciences, 2179, Springer Verlag, 2001, 95–103.
- [7] I. Gustafsson. An incomplete factorization preconditioning method based on modification of element matrices. *BIT* **36**: 1, 86–100, 1996.

- [8] D. Malkus, T. Hughes. Mixed finite element methods. Reduced and selective integration techniques: a uniform concepts. *Comp. Methods Appl. Mech. Eng.*, **15**: 63–81, 1978.
- [9] S. Margenov. Displacement decomposition-MIC(0) preconditioning of linear elasticity non-conforming FEM problems. 16th IMACS World Congress 2000, Lausanne, Proceedings, 2000, 107–4.
- [10] S. Margenov, Y. Notay. Preconditioning of non-conforming FEM systems; Performance analysis. In: O. Axelsson et al. (Eds.), *High Performance Computing in Geosciences*. Proceedings of HIPERGEOS II Workshop, 1999, 45–56.
- [11] R. Rannacher, S. Turek. Simple nonconforming quadrilateral Stokes Element. *Numerical Methods for Partial Differential Equations*, **8**: 2, 97–112, 1992.
- [12] P. Saint-George, G. Warzee, R. Beauwens, Y. Notay. High performance PCG solvers for FEM structural analyses. *Int. J. Numer. Meth. Eng.*, **39**: 1313–1340, 1996.

*Department of Structural Mechanics,
Budapest University of Technology and Economics,
H-1521 Budapest, Műegyetem rkp. 3, Hungary
*gaspard@p-mech.mech.bme.hu, **nrmeth@math.sztaki.hu*

(Received April 2, 2003)

A discrete model consisting of N straight links and N springs is defined. The originally straight model is bent into a discrete form, then it is twisted. The C_1 symmetric shapes can be determined by four parameters, and there are three constraints. The equilibrium paths are determined by the simplex method (piecewise linear approximation). Global bifurcation diagrams, spatial equilibrium shapes and periodic solutions are analyzed.

1. INTRODUCTION

Let us consider a rod with circular cross-section of radius r . The rod is long (i.e. $L \gg r$, where L is the length of the rod) and initially straight. The rod is made of a homogeneous, linear elastic material with the modulus of elasticity E and the shear modulus of elasticity G . Bending stiffness is characterized by the constant $A = EI$, where $I_x = \frac{\pi r^4}{4}$, and the twist stiffness by $C = GJ$, where $J_x = \frac{\pi r^4}{2}$. The rod is supposed to be inextensible and unshearable. Recently many publications [1–5, 8, 10, 11] deal with the following problem: first the rod is bent to a curve with a pair of moments acting on its end-sections. Then the end-sections are twisted around the rod axis, continuously providing their contact. The increasing twist rate causes stichity loss at a special value, and then spatial equilibrium states are observable.

This model is widely used as a mechanical model of DNA molecules, but several simplifications are made. In one of these simplifications the rod is treated as penetrable, i.e. we do not deal with the contact problem. The symmetry properties of such solutions are classified by Domokos [4]. When the impenetrable rod is examined, the situation is sophisticated. In simple cases contact points, at higher values of twist rate contact lines and points arise [1]. There is an interval of twist rate, where only contact line arises [8]. The contact can even break the symmetries shown by Domokos. Not all of the equilibrium states are stable, of course. The stability of solutions was examined by Coleman et al. [1].

The explicit solution of the system of differential equations of the elastic rod is given by Swigon et al. [10]. This solution is expressed in terms of elliptic integrals, what makes its handling relatively difficult, if we need the co-ordinates of all points of the rod-axis. (This is the case e.g. if we are looking for contact points). The extension of the solution to shearable or extensible rod is also complex. The DNA itself build up from discrete base pairs, which can be modeled by linear elements connected by springs. (Discrete models give good approximations to the solution of the continuous model, however the solution set is often richer, than that of the continuous model. A good example is shown in [9], where Euler's rod was examined.) A naturally discrete model of the DNA n-ring is developed by Coleman et al. in [2].